

# ASCA Observation of the Galactic Jet Source XTE J0421+560 (CI Cam) in Outburst

Y. Ueda<sup>1</sup>, M. Ishida<sup>1</sup>, H. Inoue<sup>1</sup>, T. Dotani<sup>1</sup>, J. Greiner<sup>2</sup>, W.H.G. Lewin<sup>3</sup>

## ABSTRACT

We observed the newly discovered Galactic jet source XTE J0421+560 (= CI Cam) with *ASCA* from 1998 April 3.3 to April 4.1 (UT), three days after the beginning of the outburst. The X-ray intensity in the 1–10 keV band gradually decreased with an e-folding time of about 30 hours; the decline was accompanied by spectral softening. Two flare-like intensity enhancements were detected below  $\sim 1$  keV. We could fit the average spectrum above 0.8 keV with a two-temperature model (5.7 and 1.1 keV) of thermal emission from an optically thin ionization-equilibrium plasma. The broad iron-K profile, however, requires an extra emission line at 6.4 keV, or Doppler broadening (or both). The former can be explained in terms of reflection from cold matter, while the latter can be attributed to emission from the twin jets. In both cases, the time evolution of the emission measure and of the temperature are difficult to explain by emission from a single plasma, suggesting that heat input and/or injection of material was occurring during the outburst.

*Subject headings:* stars: individual (CI Cam, XTE J0421+560) — X-rays: stars

---

<sup>1</sup>Institute of Space and Astronautical Science, Yoshinodai 3-1-1, Sagami-hara, Kanagawa 229-8510, Japan

<sup>2</sup>Astrophysikalisches Institut Potsdam, An der Sternwarte 16, 14482 Potsdam, Germany

<sup>3</sup>Department of Physics, Center for Space Research, Massachusetts Institute of Technology, Cambridge, MA 02139, U.S.A

## 1. Introduction

XTE J0421+560 is an X-ray transient discovered by the All Sky Monitor (ASM) on board the *Rossi* X-ray Timing Explorer (*RXTE*) on 1998 March 31.6 (Smith *et al.* 1998). After the detection, its X-ray intensity (2–12 keV) rapidly rose and reached a peak of about 2 Crab on 1998 April 1.04–1.08 (UT), and decayed with an e-folding time of 0.6 day (Belloni *et al.* 1998). The hard X-rays in the 20–70 keV band were also detected with BATSE on board *CGRO*, accompanied with a similar intensity evolution (Harmon, Fishman, & Paciesas 1998).

Subsequent radio and optical observations identified XTE J0421+560 with the previously known symbiotic star CI Cam(= MWC 84, see e.g., Downes 1984). On April 1.9 and 2.6, a new variable radio source was detected in the ASM X-ray error box with the Very Large Array (VLA), at a position that coincides with CI Cam (Hjellming & Mioduszewski 1998a; 1998b). Optical observations revealed brightening of CI Cam by 3.5 magnitude in the R-band (Robinson *et al.* 1998), and the presence of a He II emission line in its spectra (Wagner & Starrfield 1998; Garcia *et al.* 1998). More interestingly, VLA images taken on April 5.1 and 6.9 showed nearly symmetric twin jets (Hjellming and Mioduszewski 1998c) that were similar to those of SS 433 (Margon 1984), expanding with an apparent velocity of  $0.15c$  ( $c$  is the light speed) for an assumed distance of  $d = 1$  kpc (see Bergner *et al.* 1995).

The outburst of this new Galactic jet source, characterized by a rapid rise and decay, is unusual among other X-ray transients (Chen, Shrader, & Livio 1997). In this paper, we report results from *ASCA* observations of XTE J0421+560, performed about 3 days after the onset of the outburst. We discuss the origin of the X-ray emission and implications for its relation to the jets.

## 2. Observation and Analysis

Following the discovery by *RXTE*, we observed XTE J0421+560 with the *ASCA* satellite (Tanaka, Inoue, & Holt 1994) from 1998 April 3.31 (= MJD 50906.31) to April 4.14 as a Target of Opportunity (TOO) observation (Ueda *et al.* 1998). The GIS (Ohashi *et al.* 1996) was operated in the pulse-height mode and the SIS (Burke *et al.* 1994) was in the bright mode. A net exposure of 39,000 sec was achieved after standard data selection. The time-averaged GIS

count rate corrected for dead time was  $20 \text{ c s}^{-1}$  per sensor ( $r < 6'$ ).

Figure 1 shows the light curve in three energy bands, 0.5–1 keV, 1–4 keV, and 4–10 keV, together with the spectral hardness ratio between the 1–4 keV and 4–10 keV bands. Here, we used the GIS data for the 1–4 and 4–10 keV bands, but used the SIS data for the 0.5–1 keV band, considering its superior detection efficiencies in that band. The intensities above 1 keV gradually decreased, accompanied by a slight spectral softening. Using the GIS count rate in the 1–10 keV range, we obtained an e-folding decay time of  $30.4 \pm 0.3$  hours. On the other hand, two flare-like enhancements are noticed in the 0.5–1 keV band, which began around April 3 19:00 and April 4 1:00. The behavior of these flares seem to be completely independent of the light curves above 1 keV, suggesting a different origin from the steadily decaying emission.

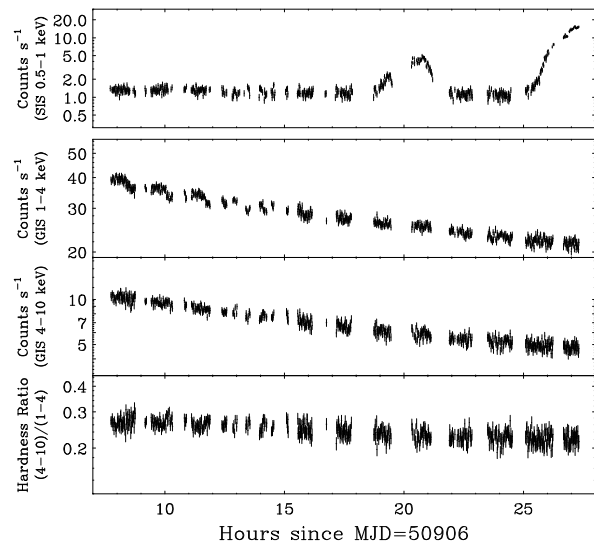


Fig. 1.— Light curves of XTE J0421+560 obtained with *ASCA* in three energy bands, 0.5–1 keV (1st panel), 1–4 keV (2nd panel), and 4–10 keV (3rd panel), and the spectral hardness ratio between the 1–4 keV and 4–10 keV bands (4th panel), binned at 64 s. The count rate of SIS1 within a selected region is plotted for the 0.5–1.0 keV band, while the sum of the GIS2 and GIS3 count rates, within a radius of  $6'$ , are shown for the other bands. Dead-time corrections were performed for the GIS data.

We first examined spectra averaged over the whole observation including the times of the soft flares (ex-

cept from April 4 2:40 to 3:20 for the SIS, when the telemetry saturation is significant.) We neglected the background, which is negligible (0.02%) compared with the source flux. We limited the energy range of the GIS spectrum used in the spectral fitting to 3.2–10 keV, in order to avoid possible uncertainties in the low energy response (Ishisaki *et al.* 1998).

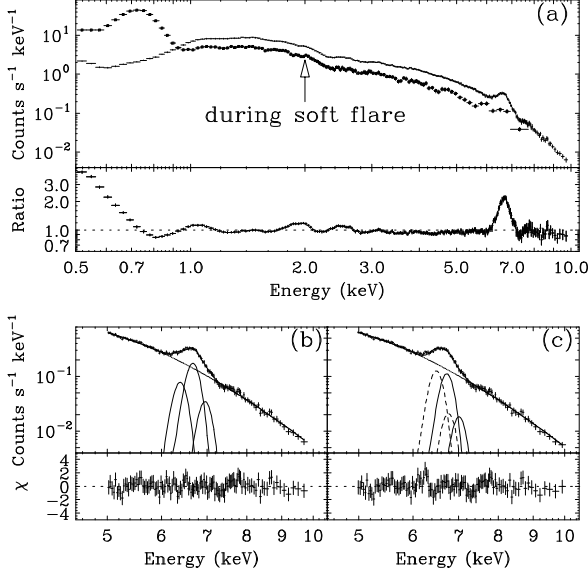


Fig. 2.— (a): The SIS folded spectrum of XTE J0421+560 (SIS0+SIS1) averaged from 1998 April 3 7:30 to April 4 2:40 (no symbol). Lower panel shows the ratio of the data to the best-fit thermal bremsstrahlung model determined in the 0.8–10 keV band. The spectrum taken from April 4 2:40 to 3:20 is plotted with square symbols. (b): The fitting results of the SIS spectrum in the 5–10 keV band with a thermal bremsstrahlung spectrum plus 3 narrow lines. The model of each component is plotted separately. We fixed the line energies at 6.4 keV, 6.68 keV, and 6.96 keV. The residuals are plotted in the lower panel. (c): Same as (b) but with 4 narrow lines, consisting of 2 red-shifted lines (dashed curves) and 2 blue-shifted lines with rest energies of 6.68 keV and 6.96 keV. The line-intensity ratio between the 6.96 keV and the 6.68 keV lines are fixed at 0.2, which is expected from a plasma with a temperature of about 6 keV.

Figure 2 (a) shows the time-averaged raw (folded) spectrum of the SIS (SIS0+SIS1). In the lower panel we show the ratio of the data fit to a simple continuum model in the 0.8–10 keV range. For the continuum, we adopted a thermal bremsstrahlung spec-

trum with interstellar absorption. We can see a soft-excess below 0.8 keV, which is attributable to the soft-flares. Above 0.8 keV, on the other hand, a strong emission-line feature is clearly seen around 6.7 keV, which probably corresponds to iron K lines. Also, the humps around 1.2 keV, 1.9 keV and 2.5 keV are suggestive of the iron L-line forest, K-lines from silicon (1.86 keV for Si XIII and 2.01 keV for Si XIV) and sulfur (2.45 keV for S XIV and 2.62 keV for S XV), respectively.

As the spectral features discussed above are probably of an optically-thin thermal plasma origin, we attempted to fit the SIS spectrum in the 0.8–10 keV range and the GIS spectrum in the 3.2–10 keV range simultaneously with an ionization-equilibrium plasma emission model given by Raymond & Smith (1977, hereafter RS model), corrected for interstellar absorption. We set elemental abundances of Si, S, and other elements as three free parameters, while that of He is fixed at the Solar value. A single temperature RS model, however, could not reproduce the data ( $\chi^2/\nu = 1578/762$  for an obtained temperature of 5.4 keV). Significant structures remained around 2 keV, 2.5 keV, and 6.4 keV in the residuals.

The poor fit in the Si and S K-bands arises because their observed line-intensity ratio between helium-like and hydrogen-like ions can not be produced by a plasma with a temperature of  $\sim 5$  keV. More directly, we determined these ratios by fitting the spectra with a model consisting of the lines from H-like and He-like ions (modeled by narrow Gaussians) and a continuum (modeled by a thermal bremsstrahlung spectrum). The obtained ratios,  $0.69 \pm 0.12$  for (Si XIV / Si XIII) and  $0.54 \pm 0.18$  for (S XIV / S XV), indicate corresponding ionization-equilibrium temperatures of  $1.2 \pm 0.2$  keV and  $1.6 \pm 0.3$  keV, respectively (Mewe, Gronenschild, & van den Oord 1985). This suggests that the observed emission originates from a multi-temperature plasma. It is supported by a great improvement in the fit with a two-temperature RS model (hereafter 2T-RS model), which gives  $\chi^2/\nu = 1232/760$  for obtained temperatures of  $5.7 \pm 0.1$  keV and  $1.06 \pm 0.02$  keV.

The 2T-RS model, however, still could not reproduce the line profile in the iron K-band, leaving large positive residuals at  $\sim 6.4$  keV. This suggests (I) the presence of an unresolved line around 6.4 keV, and/or (II) Doppler broadening, which could be attributed to the jets. Accordingly, we fit the SIS spectrum in the 5–10 keV band with two simplified models:

(I) a thermal bremsstrahlung spectrum plus 3 narrow lines at 6.4 keV, 6.68 keV ( $K\alpha$  from Fe XXV), and 6.96 keV ( $K\alpha$  from Fe XXVI), and (II) a thermal bremsstrahlung spectrum plus 4 narrow lines, consisting of 2 red-shifted lines and 2 blue-shifted lines with rest energies of 6.68 keV and 6.96 keV. Both models can reproduce the iron line profile (Figure 2(b) and 2(c)). We applied the following models to the whole spectra: (Model I) 2T-RS model with a narrow emission line around 6.4 keV, and (Model II) 2T-RS model consisting of two components with common spectral parameters (with the same normalizations, assuming that Doppler boosting is negligible), each modified by a red-shift and a blue-shift. We found that both models gave acceptable fits ( $\chi^2/\nu = 619/759$  for Model I and  $658/759$  for Model II). Two temperatures are still necessary for Model II in order to explain the line profiles of Si and S. The best fit parameters are summarized in Table 1. From Model I, we obtained an energy of  $6.41 \pm 0.04 \pm 0.06$  keV and an equivalent width of  $90 \pm 11 \pm 30$  eV for the narrow line (the second error represents the systematic error due to the uncertainty in the absolute gain (1%, Makishima *et al.* 1996)). The line center energy is consistent with that of  $K\alpha$  from cold iron. Model II gave redshift parameters (defined as  $\delta\lambda/\lambda$ ) of  $z_+ = 0.029(\pm 0.002 \pm 0.010)$  for the red-shifted component, and  $z_- = -0.007(\pm 0.002 \pm 0.010)$  for the blue-shifted component.

Since the spectrum evolves in time (see Figure 1), we divided the observation into four epochs (April 3 7:00 – 12:00, 12:00 – 18:00, 18:00 – 23:00, and April 3 23:00 – April 4 3:20) and examined their spectra above 0.8 keV separately. We fit them with Model I, fixing the elemental abundances at the best-fit values obtained from the averaged spectra (Table 1). Figure 3 shows the time history of the temperatures and emission measures separately for the high and low temperature components. We also calculated the summed emission measure from the two components and their mean temperature ( $T$ ) weighted with the emission measure, as representative parameters for the plasma in each epoch. The results are plotted in Figure 3.

Figure 3 clearly indicates that both the summed emission measure,  $E$ , and the mean temperature,  $T$ , decreased with time. To be quantitative, we fit these curves in a form of  $E(t) \propto t^{-\alpha}$  and  $T(t) \propto t^{-\beta}$ , where  $t$  is defined as a time in units of hours since the beginning of the outburst ( $t_0$ ). Assuming  $t_0$

to be March 31.6 (the onset of the X-ray outburst, Belloni *et al.* 1998), we obtained  $\alpha = 2.39 \pm 0.23$  and  $\beta = 0.95 \pm 0.16$ . The best-fit curves are plotted with dashed lines in Figure 3. When we take  $t_0$  to be April 1.04 (the peak of the X-ray outburst), the indices become  $\alpha = 2.05 \pm 0.20$  and  $\beta = 0.82 \pm 0.14$ , respectively.

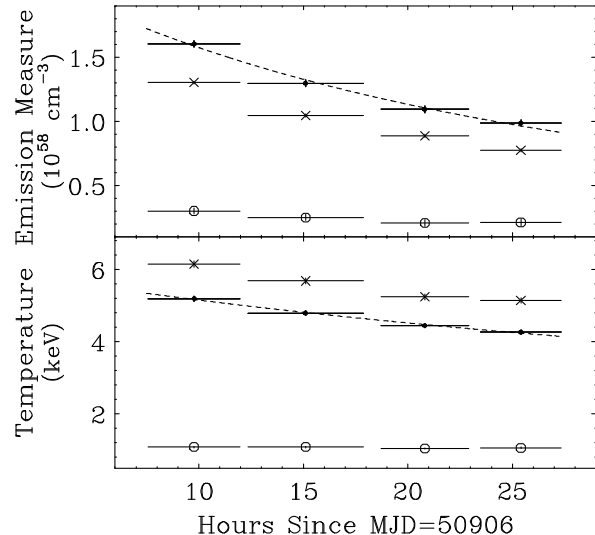


Fig. 3.— History of the emission measures (in units of  $10^{58}(d/1\text{kpc})^2 \text{ cm}^{-3}$ ) and the temperatures, derived from the 2T-RS model. Crosses and open circles represent those for the high- and the low-temperature components, respectively. The sum of two emission measures and the averaged temperature weighted with the emission measure are plotted with small filled circles. The dashed lines represent the best-fit models in the form of a power law as a function of time since the onset of the outburst (March 31.6).

Finally, we made the SIS spectrum in the epoch from April 4 2:40 to 3:20, when the soft-flare was the most prominent, in order to study the origin of the soft flares (Figure 2(a)). The soft-excess component over the extrapolation from higher energies is found to have a sharp cut-off around 0.8 keV. We could fit it with an absorbed blackbody model modified with two deep absorption edges, although it is hard to reject other possibilities (e.g., the superposition of multiple lines) due to the limited energy resolution. We obtained a temperature of  $0.12 \pm 0.02$  keV, an unabsorbed bolometric luminosity of  $(1.7^{+2.0}_{-0.4}) \times 10^{37} (d/1\text{kpc})^2 \text{ erg s}^{-1}$ , the hydrogen column density (in excess of the interstellar absorption) of  $N_{\text{H}} =$

$(2.1_{-0.4}^{+1.2}) \times 10^{21} \text{ cm}^{-2}$ , and edge energies of  $0.77 \pm 0.02$  keV and  $0.84 \pm 0.03$  keV with optical depths of  $2.3_{-0.7}^{+1.1}$  and  $26 \pm 6$ , respectively. The radius of the emitting region is then estimated at  $(1.4_{-0.2}^{+0.8}) \times 10^8 (d/1\text{kpc}) \text{ cm}$ .

### 3. Discussion

We have shown that the overall spectrum of XTE J0421+560 in the 0.8–10 keV range can be represented by the emission from an optically-thin thermal plasma with at least two temperatures. A modification is necessary, however, to account for the broad iron-K line profile. We thus propose two models (Model I and II), which cannot be distinguished from the data.

If Model I is correct, we need to explain the large ( $\sim 90$  eV) equivalent width (E.W.) of the 6.4 keV line. A fluorescence iron line with an E.W. of  $\sim 100$  eV can be produced if cold matter spherically surrounds the X-ray emitter with a column density of  $N_{\text{H}} \sim 10^{23} \text{ cm}^{-2}$  (e.g., Inoue 1985). This situation is unlikely, because the observed column density is at most  $5 \times 10^{21} \text{ cm}^{-2}$ , unless we were seeing less than 5% of the direct component. Another possibility is that we see the reflection from optically-thick cold matter. The observed E.W. can then be explained if the solid angle of the reflector seen from the emitter,  $\Omega$ , is  $\sim 2\pi$  (e.g., Basko 1978). In this case, we should see an accompanying reflection component, which has an absorption edge structure above 7.1 keV (e.g., Lightman & White 1988; George & Fabian 1991). Applying the standard edge model with Model I, we found that the presence of an absorption edge at  $7.1 \pm 0.2$  keV is allowed with an optical depth of  $0.06 \pm 0.02$ , which roughly corresponds to  $\Omega = 2\pi \sim 4\pi$  (Lightman & White 1988).

Based on Model I, we first examine the situation that a static plasma was cooling down by radiation. In this case, the decay time-scale of the emission,  $\tau$ , is given by that of the radiative cooling,  $kT/n\Lambda(T)$ , where  $T$  is the temperature,  $n$  is the number density (assumed to be common for electrons and ions), and  $\Lambda(T)$  is the emissivity of the plasma. Using  $\tau \sim 30$  hours and  $kT \sim 10$  keV, we obtain  $n \sim 10^{10} \text{ cm}^{-3}$ . Combined with the observed emission measure ( $n^2V \sim 10^{58} \text{ cm}^{-3}$ ), the size of the plasma,  $r \sim V^{1/3}$ , is estimated at  $\sim 10^{13} \text{ cm}$ . This seems to be too large, however, to find the origin of the reflector in the system of a compact object (e.g., surface of a white dwarf), which must cover the plasma with  $\Omega \sim 2\pi$ . Thus, to make this picture consistent, input of heat

and/or material into the plasma must be considered.

If Model II applies (this means XTE J0421+560 is a second example of a Galactic jet source where we directly see the X-ray emission from the jets, as is the case for SS 433), we can constrain the geometry of the jets, using the redshift parameters derived from the spectral fitting. The redshift parameters,  $z_+$  (redshifted component) and  $z_-$  (blue-shifted component), are expressed as  $z_{\pm} (\equiv \frac{\Delta\lambda_{\pm}}{\lambda}) = \gamma(1 \pm \frac{v}{c} \cos \theta) - 1$ , where  $v$  is the velocity of jets (assumed to be the same for the twin jets),  $\gamma \equiv [1 - (v/c)^2]^{1/2}$  is the Lorentz factor, and  $\theta$  is the angle between the line of sight and the axis of the jet. Their mean value,  $(z_+ + z_-)/2 = \gamma - 1$ , gives the traverse Doppler effect (time dilation). Our result in Table 1 yields  $(z_+ + z_-)/2 = (1.1 \pm 0.2 \pm 1.0) \times 10^{-2}$ , which corresponds to  $v = 0.15_{-0.11}^{+0.06}c$ . The quantity  $(z_+ - z_-)/2 = \gamma (v/c) \cos \theta$  can be used to constrain  $\theta$ . The observed value,  $(1.8 \pm 0.2 \pm 0) \times 10^{-2}$ , indicates  $\cos \theta = 0.12 \pm 0.02$ , hence  $\theta = (83 \pm 2)^\circ$ , assuming  $v = 0.15c$ .

The energy conservation equation for an expanding plasma which is uniform and isothermal is represented by:

$$\frac{dU}{dt} = -\Lambda(T) n^2 V - nkT \frac{dV}{dt},$$

where  $k$  is the Boltzmann constant,  $V$  is the volume,  $U = (3/2)nkTV$  is the total energy in the plasma (here we have assumed a constant velocity), and  $\Lambda(T)$  is the emissivity of the plasma. The first term on the right represents the radiative cooling, while the second represents the adiabatic cooling. First, we assume that the total number of electrons in the plasma,  $N (\equiv nV)$ , is conserved. To compare this with the previous analysis, we represent the time dependence of the emission measure and the temperature in a form of  $E(t) \propto t^{-\alpha}$  and  $T(t) \propto t^{-\beta}$ , where  $t$  is the time since the expansion started. This yields  $n \propto t^{-\alpha}$ , and  $V \propto n^{-1} \propto t^{\alpha}$ . Note that  $\alpha = 3$  corresponds to the 3-dimensional self-similar free expansion. Finally, the energy conservation equation becomes:

$$-\frac{3}{2}\beta \frac{kT}{t} = -n\Lambda(T) - \alpha \frac{kT}{t}.$$

We found, however, that this equation cannot be satisfied for the observed values of  $\alpha = 2.39 \pm 0.23$  and  $\beta = 0.95 \pm 0.16$ , because the left term is always smaller than the second term on the right. This implies that the plasma we observed is not a single, freely expanding plasma. Injection of new (hot) material, and/or heat input, such as irradiation from the com-

compact star, are required to prevent the observed temperature from cooling fast. An example of the former can be found in the cooling jet model applied to SS 433 (Kotani 1997).

The origin of the soft flares seems to be independent of that of the thin thermal emission discussed above. The spectrum of the soft flares are similar to that observed from the super soft sources (SSSs, see e.g., Greiner 1996). The apparent edges might be attributable to those of O VII (0.74 keV) and O VIII (0.87 keV) (Ebisawa *et al.* 1996). However, a temperature as high as 120 eV and the rapid time variability on a time scale of 1 hour have not been observed from the SSSs. We leave it for future studies to find out what the soft flares are and what causes the soft flares.

In summary, we revealed that the X-ray emission from XTE J0421+560 came from a multi-temperature thin-thermal plasma. The iron line profile suggests the presence of a reflection component and/or the interesting possibility that this emission is produced in the twin jets, as is the case for SS 433. It will be of great interest to examine this further with radio data.

We thank members of the ASCA team for making this TOO observation possible, and Y. Tanaka for useful discussions. JG is supported by the German Bundesministerium für Bildung, Wissenschaft, Forschung und Technologie (BMBF/DLR) under contract No.FKZ 50 QQ 9602 3. WHGL is grateful to NASA for support.

## REFERENCES

- Anders, E. & Grevesse, N. 1989, *Geochimica et Cosmochimica Acta*, 53, 197
- Basko, M.M. 1978, *ApJ*, 223, 268
- Bergner, Y.K., *et al.* 1995, *A&AS*, 112, 221
- Burke, B.E., Mountain, R.W., Daniels, P.J., Cooper, M.J., Dolat, V.S. 1994, *IEEE trans. nucl. sci.* 41, 375
- Chen, W., Shrader, C.R., & Livio, M. 1997, *ApJ*, 491, 312
- Downes, R.A. 1984, *PASP*, 96, 807
- Ebisawa, K. *et al.* 1996, in *Supersoft X-ray Sources (Lecture Notes in Physics)*, ed. J. Greiner (Springer), p91
- Garcia, M.R., *et al.* 1998, *IAU Circ.*, No. 6865
- George, I.M. & Fabian, A.C. 1991, *MNRAS*, 249, 352
- Greiner, J. 1996, *Supersoft X-ray Sources (Lecture Notes in Physics)*, (Springer)
- Harmon, B.A., Fishman, G.J., & Paciesas, W.S. 1998, *IAU Circ.*, No. 6874
- Hjellming, R.M., & Mioduszewski, A.J. 1998a, 1998b, & 1998c, *IAU Circ.*, No. 6857, 6862, & 6872
- Inoue, H. 1985, *Space Science Reviews*, 40, 317
- Ishisaki, Y. *et al.* 1998, in preparation
- Kotani, T. 1997, Ph.D. thesis, Univ. of Tokyo
- Belloni, T. *et al.* 1998, in preparation
- Lightman, A.P. & White, T.R. 1988, *ApJS*, 335, 57
- Mewe R., Gronenschild E.H.B.M., & van den Oord G.H.J., 1985, *A&AS*, 62, 197.
- Makishima, K. *et al.* 1996, *PASJ*, 48, 171
- Margon, B. 1984, *ARA&A*, 22, 507.
- Ohashi, T. *et al.* 1996, *PASJ*, 48, 157
- Raymond, J.C., & Smith, B.W. 1977, *ApJS*, 35, 419
- Robinson, E.L., Welsh, W.F., Adams, M.T., Cornell, M.E. 1998, *IAU Circ.*, No. 6862
- Smith, D., Remillard, R., Swank, J., Takeshima, T., & Smith, E. 1998, *IAU Circ.*, No. 6855
- Tanaka, Y., Inoue, H., & Holt, S.S. 1994, *PASJ*, 46, L37
- Ueda, Y., *et al.* 1998, *IAU Circ.*, No. 6872
- Wagner, R.M. & Starrfield, S.G. 1998, *IAU Circ.*, No. 6857

TABLE 1  
RESULTS OF THE SPECTRAL FITS

	Model I <sup>a</sup>	Model II <sup>b</sup>
$N_{\text{H}}$ ( $10^{21} \text{ cm}^{-2}$ )	$4.6 \pm 0.3$	$4.3 \pm 0.3$
$T_1$ (keV)	$5.68 \pm 0.11$	$5.65 \pm 0.08$
$\text{EM}_1^{\text{c}}$	$0.83 \pm 0.02$	$0.83 \pm 0.02$
$T_2$ (keV)	$1.07 \pm 0.03$	$1.10 \pm 0.04$
$\text{EM}_2^{\text{c}}$	$0.21 \pm 0.03$	$0.14 \pm 0.03$
Si Abundance <sup>d</sup>	$1.25 \pm 0.15$	$1.67 \pm 0.19$
S Abundance <sup>d</sup>	$1.03 \pm 0.13$	$1.29 \pm 0.16$
Others Abundance <sup>d</sup>	$0.36 \pm 0.02$	$0.46 \pm 0.02$
Line Energy (keV)	$6.41 \pm 0.04 \pm 0.06^{\text{e}}$	...
Equivalent Width (eV)	$90 \pm 11 \pm 30^{\text{e}}$	...
$z_+^{\text{f}}$	...	$2.9 \pm 0.2 \pm 1.0^{\text{e}}$
$z_-^{\text{f}}$	...	$-0.68 \pm 0.18 \pm 1.0^{\text{e}}$
$\chi^2/\nu$	619/759	658/759

<sup>a</sup>Two-temperature Raymond & Smith plasma model with an emission line.

<sup>b</sup>Two-temperature Raymond & Smith plasma model consisting of twin Doppler-shifted components with common parameters.

<sup>c</sup>Emission measure in units of  $10^{58} (d/1\text{kpc})^2 \text{ cm}^{-3}$  (sum of the twin components for Model II).

<sup>d</sup>Relative to the Solar abundance as given by Anders & Grevesse (1989).

<sup>e</sup>The first error represents the statistical error; the second one represents the systematic error due to the uncertainty in the gain.

<sup>f</sup>Redshift parameter ( $\equiv \Delta\lambda/\lambda$ ) in units of  $10^{-2}$ .  $z_+$  and  $z_-$  correspond to the red-shifted and the blue-shifted components, respectively.

NOTE.—Errors are 90% confidence limits for a single parameter.